Study of the short-term cylinder wall temperature oscillations during transient operation of a turbocharged diesel engine with various insulation schemes

C D Rakopoulos*, **E G Giakoumis,** and **D C Rakopoulos**
Department of Thermal Engineering, National Technical University of Athens, Greece

The manuscript was accepted after revision for publication on 4 February 2008.

DOI: 10.1243/14680874JER00608

Abstract: This work investigates the phenomenon of short-term temperature (cyclic) oscillations in the combustion chamber walls of a turbocharged diesel engine during transient operation after a ramp increase in load. For this purpose, an experimentally validated simulation code of the thermodynamic cycle of the engine during transient conditions is used. This takes into account the transient operation of the fuel pump and the development of friction torque using a detailed per degree crank angle submodel, while the equations for each cylinder are solved individually and sequentially. The thermodynamic model of the engine is appropriately coupled to a wall periodic heat conduction model, which uses the gas temperature variation as boundary condition throughout the engine cycle after being treated by Fourier analysis techniques. Various insulation schemes are examined (plasma spray zirconia, silicon nitride) for load-increase transient operation. The evolution of many variables during transients is depicted, such as amplitude of oscillation, depth where the swing dies out, or gradient of temperature swing. The investigation reveals many interesting aspects of transient engine heat transfer, regarding the influence that the engine wall material properties have on the values of cyclic temperature swings.

Keywords: turbocharged diesel engine, transient operation, temperature oscillations, heat conduction, insulation, silicon nitride, plasma spray zirconia

1 INTRODUCTION – BACKGROUND ON CYLINDER WALL TEMPERATURE OSCILLATIONS

The importance of heat transfer to the combustion chamber walls of internal combustion engines has been recognized from the early stages of their development. Results from various theoretical and experimental research efforts on this subject have been presented in the literature during the last decades, as for example in references [**1**] to [**5**]. In recent years, interest in the heat transfer phenomena in internal combustion engines has greatly intensified because of their major importance on, among other things, thermal loading at critical places in the combustion chamber components. Heat transfer in internal combustion engines is extremely complex, since the relevant phenomena are of transient nature even under steady state engine operation, three-dimensional, and subject to rapid variations in cylinder gas pressure and temperatures during an engine cycle.

Moreover, during the last two decades there has been an increasing interest in the low heat rejection (LHR, or sometimes loosely termed 'adiabatic') diesel engine [**6–11**]. The objective of an LHR cylinder is to minimize heat loss to the walls, eliminating the need for a coolant system. This is achieved through the increased temperatures inside the cylinder resulting from the insulation applied to the cylinder walls, piston crown, cylinder head, or valves. By so doing, a reduction can be observed in ignition delay and thus combustion noise, and also in hydrocarbons and particulate matter emissions,

**Corresponding author: Internal Combustion Engines Laboratory, School of Mechanical Engineering, National Technical University of Athens, 9 Heroon Polytechniou St, Zografou Campus, 15780 Athens, Greece. email: cdrakops@central.ntua.gr*

while an increase in exhaust gas energy is effected. A major issue here is the decrease in the volumetric efficiency, which adversely affects the power output, and the increase in NO_x emissions [**3**]. To this aim, various researchers [**9**, **10**] have proposed the application of thin thermal barrier coatings as opposed to the thicker ones for performance improvement from insulated engines.

The (transient) temperature and heat flux variations in the combustion chamber walls can be divided into two main categories:

(a) the long-term response variations, resulting from the large time scale (of the order of seconds), non-periodic variations of engine speed and/or load;
(b) the short-term response variations, which are the result of the fluctuations of gas pressure and temperature during an engine cycle, having a time period of the order of milliseconds.

The latter are particularly pronounced when an LHR engine cylinder is under study. Assanis and Heywood [**2**] were among the first to study the development of the short-term response temperature variations in engine cylinder walls that were partially insulated with plasma spray zirconia (PSZ). They applied a single-zone model on a turbocharged and turbo-compound diesel engine, and highlighted the increased magnitude (of the order of more than 100 K) of the developed temperature oscillations during a steady state engine cycle. Rakopoulos *et al.* [**12**, **13**] extended the analysis to include the effect of silicon nitride insulation and provided comparative results for the various insulation schemes applied on a naturally aspirated diesel engine cylinder.

Some researchers (for example, references [**14**] to [**17**]) have studied the short-term temperature variations experimentally and commented on the high complexity and difficulty involved. Namely, fast response thermocouples are needed, carefully installed at strategic points in the engine structure; proper amplification and a sophisticated data acquisition system are necessary for the correct interpretation of the data obtained.

One common aspect of the above-mentioned works is that they investigated the heat transfer balance to the diesel engine cylinders during steady state engine operation. However, it is a well-known fact today that transient turbocharged diesel engine operation is of particular importance since it is often linked with off-design, e.g. turbocharger lag, and consequently non-optimum performance leading to unacceptable exhaust emissions and poor speed response [**18–20**]. Although during the last decades diesel engine modelling and experimental investigation have helped enormously towards the study and optimization of transient operation for both load and speed changes [**18–27**], the number of works committed so far to the study of the temperature variations during transient operation is extremely limited. This may be attributed to the following facts:

(a) the initial wall temperature was found to only slightly affect speed response, with the hot walls being more favourable, as now smaller amounts of exhaust gas energy are lost to the heating of cylinder walls, thus decreasing turbocharger lag [**20**, **22**, **23**];
(b) the long-term temperature variations last one to two orders of magnitude longer than the corresponding transient event.

The development of these long-term temperature variations after a load or speed change was studied by Keribar and Morel [**21**], who simulated in detail the heat transfer process separately for the piston crown, cylinder liner, cylinder head, and valves. They used a convective heat transfer submodel based on in-cylinder flow accounting for swirl, squish, and turbulence, and a radiation heat transfer submodel based on soot formation. Keribar and Morel [**21**], and also Rakopoulos *et al.* [**28**, **29**], applied finite element methods to the structure of the cylinder walls and identified the fact that the thermal shock, i.e. the sharp temperature gradient development in the engine structure after a ramp increase in load or fuelling, may take prohibitive values impairing the engine performance. This is due to the high wall thermal fatigue when materials of specific interest, for example thermal insulators, are used.

Unlike their long-term counterparts, the short-term temperature variations develop fully during each engine cycle. They can assume increased values during a transient event after a ramp increase in load, since fuelling and hence gas temperatures increase significantly in only a few seconds. Since load transients are considered to be a highly adverse engine operating condition that can lead to early material failure [**2**, **21**], it seems logical to investigate the propagation of the short-term temperature variations under the very demanding conditions induced during transient operation after a ramp increase in load.

The present investigation aims to identify the development of these short-term temperature variations during the transient operation of a

Table 1 Basic data for engine and turbocharger

	MWM TbRHS 518S
Engine model and type	In-line, six-cylinder, four-stroke, water-cooled, turbocharged and aftercooled, heavy-duty diesel engine
Speed range	1000–1500 r/min
Bore/stroke/swept volume	140 mm/180 mm/16.62 l
Compression ratio	17.7:1
Maximum power	320 HP (236 kW) at 1500 r/min
Maximum torque	1520 N m at 1250 r/min
Fuel pump	Bosch PE-P series, in-line, six-cylinder with mechanical governor Bosch RSUV 300/900
Turbocharger	KKK M4B 754/345 Single-stage, centrifugal compressor Single-stage, twin-entry, axial turbine
Moment of inertia	Engine and brake, 15.60 kg m^2 Turbocharger, 7.5×10^{-4} kg m^2

turbocharged diesel engine. The analysis will be extended to study various insulation schemes applied to the engine cylinder walls. By so doing, it is intended to shed light on the underlying complicated heat transfer mechanism and reveal the magnitude of the developed temperature gradients.

To this aim, an experimentally validated transient diesel engine simulation code has been extended to include a detailed heat transfer analysis applying Fourier techniques. The model incorporates some important features to account for the peculiarities of the transient operation. In the developed submodels, improved relations are included concerning fuel injection, combustion, friction, dynamic analysis, and multicylinder engine operation during transient conditions [**23**, **26**, **27**].

The analysis carried out will be presented in a series of diagrams that depict the response of various heat transfer variables of interest – such as gas and wall-side temperatures, heat transfer coefficient, amplitude of the temperature oscillation, and depth where the swing dies out – with respect to the engine cycles. Various schemes will be considered regarding insulation (i.e. plasma spray zirconia or silicon nitride) and cylinder wall materials (i.e. cast iron and aluminium). Owing to the narrow speed range of the engine used, only load increases under constant governor setting are investigated; these, nonetheless, play a significant role in the European Transient Cycles of heavy-duty vehicles.

2 EXPERIMENTAL STUDY

The experimental investigation was conducted on a heavy-duty, turbocharged, and after-cooled, medium–high-speed diesel engine, located at the authors' laboratory, the main data of which are given in Table 1. The first requirement from the engine test-bed instrumentation was to investigate the steady state, uninsulated performance of the examined engine. For this purpose, an extended series of trials was conducted in order on the one hand to examine the model's predictive capabilities and on the other to calibrate successfully the individual submodels. Figure 1(a) shows the comparison between experiment and simulation for the whole engine speed operating range and for various loads at steady state conditions. Brake mean effective pressure (b.m.e.p.), brake-specific fuel consumption (b.s.f.c.), boost pressure, and turbocharger speed are depicted in this figure. It is obvious that the matching between experimental and simulated results is very good for all engine operating conditions, thus providing a sound basis for a successful transient study. Figure 1(b) expands on Fig. 1(a) by showing two typical experimental versus predicted cylinder pressure diagrams for representative engine operating conditions.

For the transient tests conducted, the initial speed was 1180 or 1380 r/min, and the initial load 10 per cent of the engine full load. The final conditions for the transient events varied from 47 to 95 per cent of the engine full load [**23**]. A typical example of a transient experiment is given in Fig. 2, showing the response of some important engine and turbocharger properties. Here, the initial load was 10 per cent of the full engine load at 1180 r/min. The final load applied was almost 50 per cent of the full engine load (400 per cent relative load-change). The overall matching between experimental and predicted transient response seems fairly satisfactory for both engine and turbocharger variables regarding trends and final operating conditions of the engine. Boost pressure is delayed compared with the speed profile owing to the well-known turbocharger lag effect, which, for the particular engine-brake set-up, was less pronounced due to the relatively high mass moment of inertia.

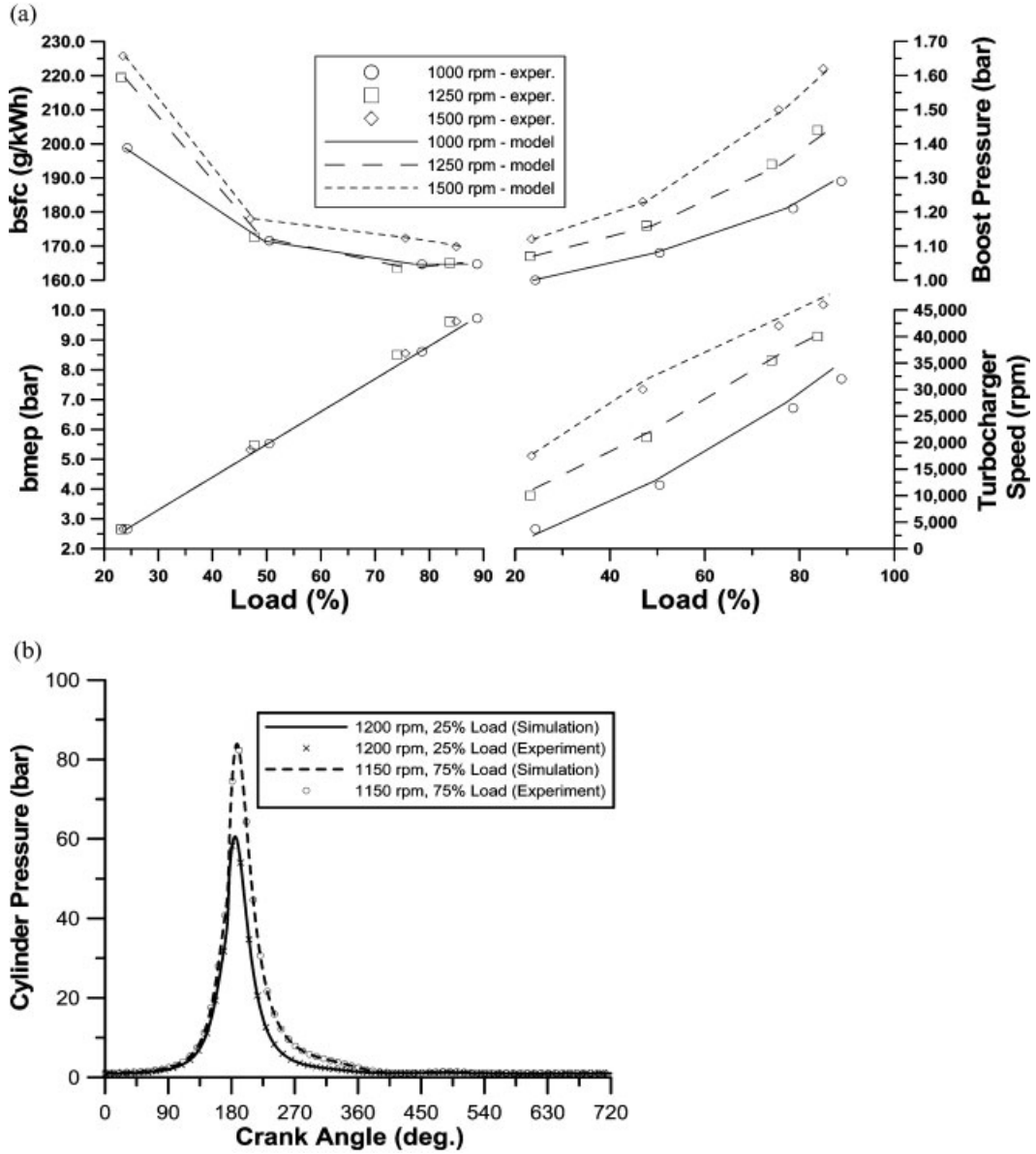

Fig. 1 (a) Experimental and predicted engine and turbocharger steady state results. (b) Comparison between measured and predicted cylinder pressure diagrams, for two typical engine, steady state, operating conditions

Some remarks concerning the matching between predicted and experimental transient results are provided below. The application of the final load was effected by the movement of the brake control lever (this task lasted 0.2 s), which in turn increased the amount of water inside the brake, by appropriately increasing the active surface of the inlet tube. Unfortunately, the hydraulic brake used in the experimental procedure is characterized by a high mass moment of inertia, of the order of 5.375 kg m^2, resulting in a long, abrupt, and non-linear actual load-change profile. The actual duration of the load application was accounted for in the simulation model by increasing the load application time. The non-linear character of the load application though, which could not be accounted for in the simulation, is responsible for the differences observed between experimental and simulated results in Fig. 2.

3 SIMULATION ANALYSIS

3.1 General process description

The present analysis does not, at present, include prediction of exhaust gas emissions and on the other hand deals with transient operation calculations on

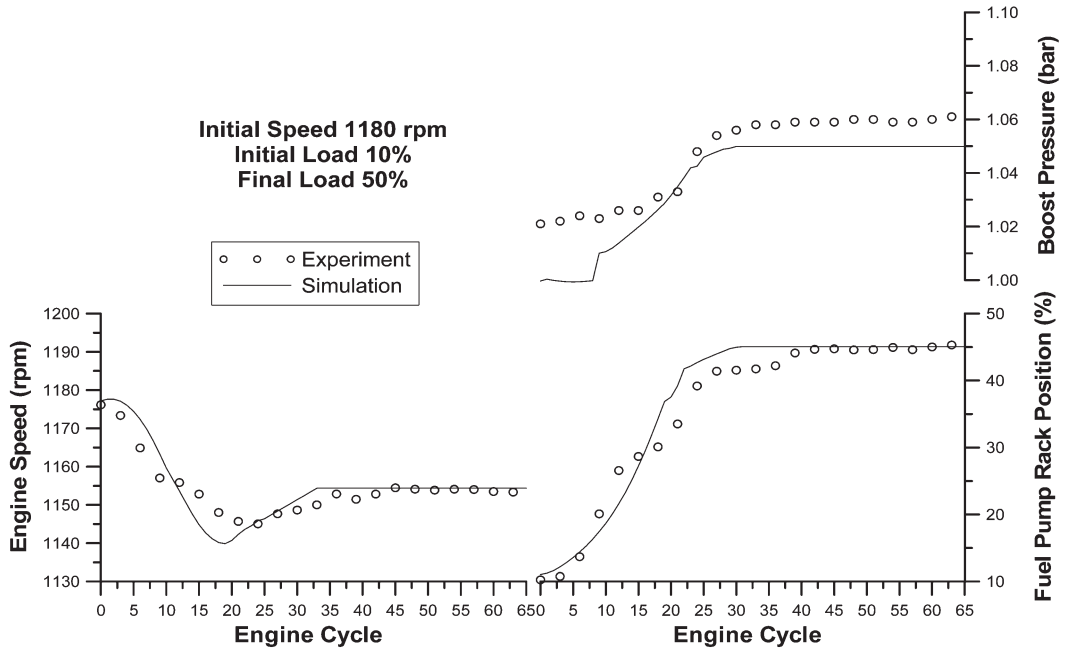

Fig. 2 Experimental and predicted engine transient response to an increase in load

a degree crank angle (°CA) basis. To this aim, a single-zone model is used for the simulation of the thermodynamic processes following the filling and emptying modelling technique. This approach combines satisfactory accuracy with limited PC program execution time.

3.2 In-cylinder processes

For studying the combustion process, the model proposed by Whitehouse and Way [**30**] is applied. It is vital for a proper simulation of transient response that combustion modelling takes into consideration the continuously changing nature of operating conditions. Thus, constant K in the (dominant) preparation rate equation of the Whitehouse–Way model is correlated with the Sauter mean diameter (SMD) of the fuel droplets through a formula of the type $K \infty (1/\mathrm{SMD})^2$ [**4**].

The improved model of Annand and Ma [**1**] is used to simulate the heat loss Q_L to the cylinder walls

$$\frac{\mathrm{d}Q_L}{\mathrm{d}t} = A\left\{\frac{k_g}{D} Re^b \left[a\left(T_g - \bar{T}_{w,g}\right) + \frac{a'}{\omega}\frac{\mathrm{d}T_g}{\mathrm{d}t}\right] + c\left(T_g^4 - \bar{T}_{w,g}^4\right)\right\} = h_g\left(T_g - \bar{T}_{w,g}\right) \quad (1)$$

where a, a', b, and c are constants evaluated after the experimental matching at steady state conditions, k_g is the gas thermal conductivity (a function of its temperature), and the Reynolds number Re is calculated with a characteristic speed derived from a k–ε turbulence model and a characteristic length equal to the piston diameter D.

The temperature $\bar{T}_{w,g}$ used above corresponds to the mean, over an engine cycle, gas-side cylinder liner temperature, which changes from cycle to cycle during the transient event. For the piston crown, the temperature is always assumed to be 50 K higher and for the cylinder head 100 K higher than the current temperature of the liner.

3.3 Wall periodic heat conduction model

In the present study a detailed heat transfer mechanism scheme is applied for the engine cylinder; by so doing, the temperature distribution and the respective heat flux are studied from the gas to the cylinder wall up to the coolant (convection from the gas to the internal wall surface and from the external wall surface to the coolant, and conduction across the insulated cylinder wall). The following usually applied and well-justified assumptions are made concerning the wall temperature computation:

(a) all cylinder surfaces are at a constant temperature throughout an engine transient cycle (changing from cycle to cycle);

(b) heat transfer by conduction through the walls is one dimensional;
(c) the properties of the cylinder wall and the insulators remain constant with temperature and time;
(d) the coolant temperature, T_c, is constant and known *a priori*.

The heat transfer rate from the gas to the walls is a harmonic function of time, with a period of one engine cycle. As a result of this, periodic temperature waves propagate into the wall structure, but nonetheless die out at a small distance (of very few mm) from the wall inside surface, beyond which the temperature distribution is at steady state [**2**].

In order to calculate the heat transfer rate through a certain location of the combustion chamber wall, during a complete engine cycle, the unsteady heat conduction equation must be solved with the appropriate boundary conditions. The total temperature, i.e. steady state plus time-periodic, $T(x,t)$, at any point x within the wall and at any time t, should satisfy the unsteady one-dimensional heat conduction equation [**31**]

$$\frac{\partial T}{\partial t} = \alpha \frac{\partial^2 T}{\partial x^2} \tag{2}$$

where α is the wall thermal diffusivity. The solution of this equation is accomplished by decomposing the problem into its steady state and time-periodic components.

3.3.1 Steady state heat conduction problem

Applying the boundary conditions to all wall sides (gas side, coolant side, and end of insulation side) of the four-stroke diesel engine, the following equation is obtained for the general case where a layer of insulation is also present [**31**]

$$\frac{1}{4\pi}\int_0^{4\pi} \frac{\mathrm{d}Q_L}{\mathrm{d}\varphi}\mathrm{d}\varphi = A\frac{k_{ins}}{S_{ins}}\left(\bar{T}_{w,g} - \bar{T}_{w,m}\right)$$

$$= A\frac{k_w}{S_w}\left(\bar{T}_{w,m} - \bar{T}_{w,c}\right) = Ah_c\left(\bar{T}_{w,c} - T_c\right) \tag{3}$$

where $\mathrm{d}Q_L/\mathrm{d}\varphi$ is the heat flux computed from equation (1), also bearing in mind that $\mathrm{d}\varphi = 6N\,\mathrm{d}t$, S_{ins} is the thickness of the insulation layer with k_{ins} its thermal conductivity, S_w is the cylinder wall thickness with k_w its thermal conductivity, h_c is the heat transfer coefficient from the external wall side (respective temperature, $\bar{T}_{w,c}$) to the coolant; the overbar denotes mean temperatures over an engine cycle. Equation (3) is solved for the three unknown variables, i.e. the wall temperatures $\bar{T}_{w,g}$, $\bar{T}_{w,m}$, and $\bar{T}_{w,c}$, which change from cycle to cycle during the transient event but are considered to remain constant throughout each cycle, hence the 'steady state' definition.

3.3.2 Time-periodic heat conduction problem

The detailed formulation of the time-periodic heat conduction problem has been analysed by Rakopoulos *et al.* [**12**, **13**]. In this paper, only a brief outline will be given highlighting the basic equations applied. The time-periodic part, $T_p(x,t)$, at any point x within the wall and at any time t, will satisfy the unsteady one-dimensional heat conduction equation within a parallel slab having a thermal diffusivity α

$$\frac{\partial T_p}{\partial t} = \alpha \frac{\partial^2 T_p}{\partial x^2} \tag{4}$$

This continuous partial differential equation can be solved analytically [**32**] using Fourier analysis techniques, even though during transients $T_p(x,t)$ is not a periodic function. Equation (4) is subjected to the boundary condition of the inside wall surface, at $x = 0$, to be exposed to the gas temperature that varies periodically in time [**31**]

$$-k_{ins}\left.\frac{\partial T_p}{\partial x}\right|_{x=0} = \bar{h}_g\left(T_p - T_{pg}\right) \tag{5}$$

The time-periodic part of gas temperature $T_{pg}(t)$ is expressed as a Fourier series, in the following form [**3**, **33**]

$$T_{pg}(t) = \sum_{n=1}^{\infty}\left[A_n\cos\left(\frac{2\pi n}{\tau_o}t\right) + B_n\sin\left(\frac{2\pi n}{\tau_o}t\right)\right] \tag{6}$$

where τ_o is the time period of the temperature oscillation, which for a four-stroke engine corresponds to a frequency that is half the engine speed. For the wall temperature this results in [**34**]

$$T_p = \sum_{n=1}^{\infty}\frac{\exp(-\xi_n x)}{\sqrt{1+2\zeta_n+2\zeta_n^2}}\left[C_n\cos\left(\frac{2\pi n}{\tau_o}t - \xi_n x - \theta_n - \delta_n\right)\right] \tag{7}$$

where the following quantities have been defined ($k_{ins} \equiv k_w$ for a non-insulated wall case)

$$C_n = \sqrt{A_n^2 + B_n^2}, \qquad A_n = \frac{2}{\tau_o}\int_o^{\tau_o} T_g(t)\cos\left(\frac{2\pi n}{\tau_o}t\right)\mathrm{d}t,$$

$$B_n = \frac{2}{\tau_o}\int_o^{\tau_o} T_g(t)\sin\left(\frac{2\pi n}{\tau_o}t\right)\mathrm{d}t$$

$$A_o = \bar{T}_g = \frac{1}{\tau_o}\int_o^{\tau_o} T_g(t)\mathrm{d}t, \quad \delta_n = \tan^{-1}(B_n/A_n)$$

$$\xi_n = \sqrt{\pi n/\alpha\tau_o}, \quad \zeta_n = \xi_n(k_{ins}/h)$$

$$= \sqrt{\pi n k_{ins}^2/\alpha\tau_o h^2}, \quad \theta_n = \tan^{-1}\left(\frac{1}{1+(1/\zeta_n)}\right) \tag{8}$$

From equation (7), the term $C_n\cos(\xi_n x) = C_n\cos\left[\left(\sqrt{\pi n/\alpha\tau_o}\right)x\right]$ represents a cosine wave of amplitude C_n and wavelength x_o calculated from the condition $\left(\sqrt{\pi n/\alpha\tau_o}\right)x_o = 2\pi$ and $n = 1$, that is

$$x_o = \sqrt{\pi\alpha\tau_o} \tag{9}$$

3.4 Computational procedure

The computational process begins with the cylinder steady state calculations where a mean, gas-side, wall temperature is assumed. By so doing, the calculation of the heat flux from equation (1) is made possible. At the end of the first trial cycle, a balance has been carried out between the total, during the cycle, gas-to-inside wall heat transfer and the corresponding heat conducted through the walls, so that a new improved estimate of cylinder wall temperature can be computed and used for the next engine cycle iteration using equation (3). Iterations continue in this 'external loop' until calculations lead to convergence.

After the final convergence of the whole thermodynamic cycle, the transient cycles commence (provided that all other properties of interest – i.e. cylinder pressure and temperature at the beginning of the cycle, indicated mean effective pressure, etc. – have also converged). During the transient event, the mean temperatures obtained from equations (3) at the end of each cycle are used for the computation of the corresponding heat flux during the next transient cycle and so on. At the end of each transient cycle, the values of the gas temperatures in the whole cycle are used for calculating its Fourier sine and cosine coefficients. Then, the computations proceed concerning the time-periodic part of wall temperatures and the corresponding heat transfer rates, as described in the above section.

3.5 Other submodels

Various detailed submodels have been incorporated in the main code. These have been analysed in previous publications by the authors [**20**, **23**, **26**, **27**]. They deal with the following aspects of engine operation.

1. Multi-cylinder engine modelling. During transient operation, each cylinder experiences during the same engine cycle different fuellings owing to the continuous movement of the fuel pump rack initiated by the load or speed changes, and different air-mass flowrates owing to the continuous movement of the compressor operating point. These result in significant differentiations in torque response and finally speed, thus significantly affecting the whole engine operation. A multi-cylinder engine model is thus developed, i.e. one in which all the governing differential and algebraic equations are solved individually and sequentially for every one cylinder of the six-cylinder engine under study.
2. Fuel pump operation. A mathematical fuel injection model, experimentally validated at steady state conditions, is applied to simulate the fuel pump–injector lift mechanism [**35**]. It takes into account the delivery valve and the injector needle motion. The unsteady gas flow equations are solved using the method of characteristics, providing the dynamic injection timing as well as the duration and the rate of injection for each cylinder at each transient cycle at the point of the individual cylinder's static injection timing. The obvious advantage here is that the transient operation of the fuel pump is also taken into account, mainly through the fuel pump residual pressure value, which is built up together with the other variables during the transient event.
3. Friction. For the calculation of friction inside the cylinder, the method proposed by Taraza *et al.* [**36**] is adopted. It describes the non-steady profile of friction torque during each cycle based on fundamental friction analysis. In this method the total amount of friction is divided into four parts,

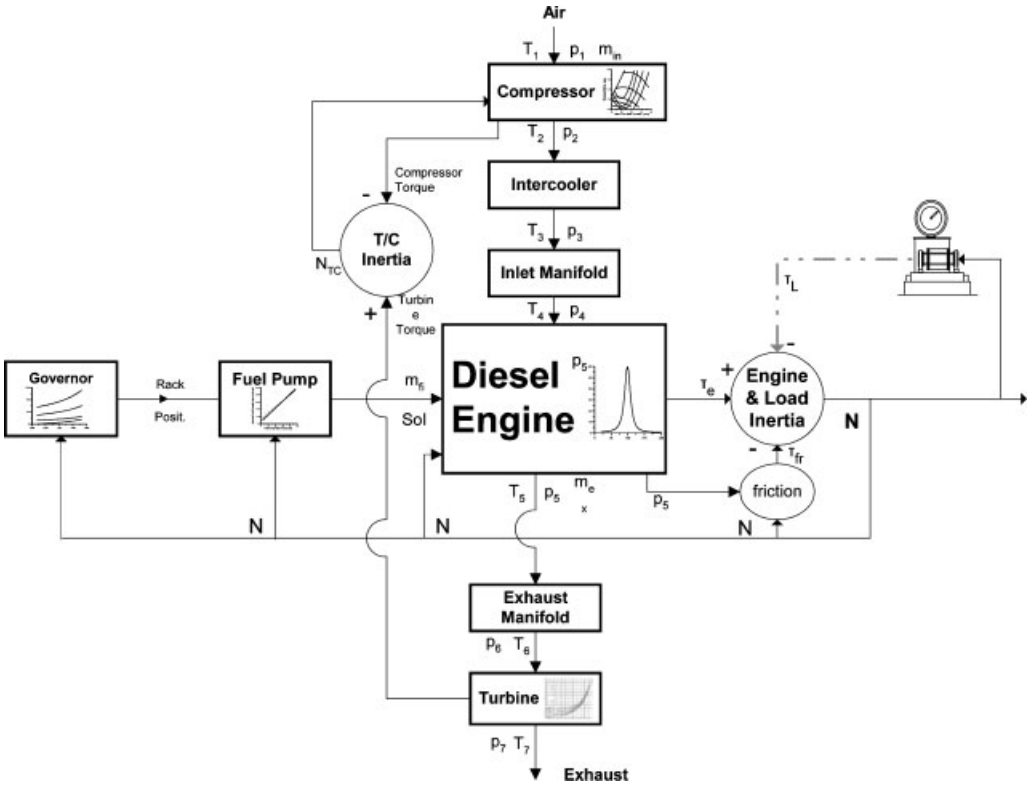

Fig. 3 Block diagram of transient simulation code

i.e. piston rings assembly, loaded bearings, valve train, and auxiliaries. Total friction torque at each degree CA is the sum of the above terms and it varies continuously during the engine cycle, unlike the usually applied 'mean' friction mean effective pressure equations where friction torque remains constant throughout each cycle.

The block diagram of the engine simulation code valid under transient conditions is depicted in Fig. 3, which shows all the interconnections between engine subsystems and between diesel engine and load.

4 INSULATION SCHEMES AND TRANSIENT SCHEDULES

The baseline, non-insulated, case configuration is that corresponding to the engine in hand, assuming a cast iron wall thickness everywhere of 10 mm. Table 2 illustrates the four, widely different, insulation schemes considered for the present study. The main thermal properties of the cylinder wall materials and insulators (ceramics) used are given in Table 3. In the present study, which concerns transient operation, for each case examined the initial load was 10 per cent of the engine maximum load at the respective conditions. The latter were defined each time from the insulation scheme applied. Afterwards, an abrupt 650 per cent relative load-change was experienced. The final conditions, after the new equilibrium is achieved in 4–5 s, roughly correspond to a 75 per cent load. The case with a 10–95 per cent load-change will also be depicted only for the cast iron–1.0 mm PSZ coating scheme, in order to enhance the importance of some of the results obtained.

Table 2 Summary of the insulation schemes studied

Scheme	Cylinder wall	Insulation	Depth of insulation
1	Cast iron	—	—
2	Cast iron	SN	4.0 mm
3	Cast iron	PSZ	1.0 mm
4	Cast iron	PSZ	1.5 mm
5	Aluminium	PSZ	1.0 mm

SN, silicon nitride.

Table 3 Thermal properties for cylinder wall materials and insulators

	Conductivity, k (W/m K)	Thermal diffusivity, α (m^2/s)
Cast iron	54	14×10^{-6}
Aluminium	180	78×10^{-6}
SN	10	2.80×10^{-6}
PSZ	1.0	0.90×10^{-6}

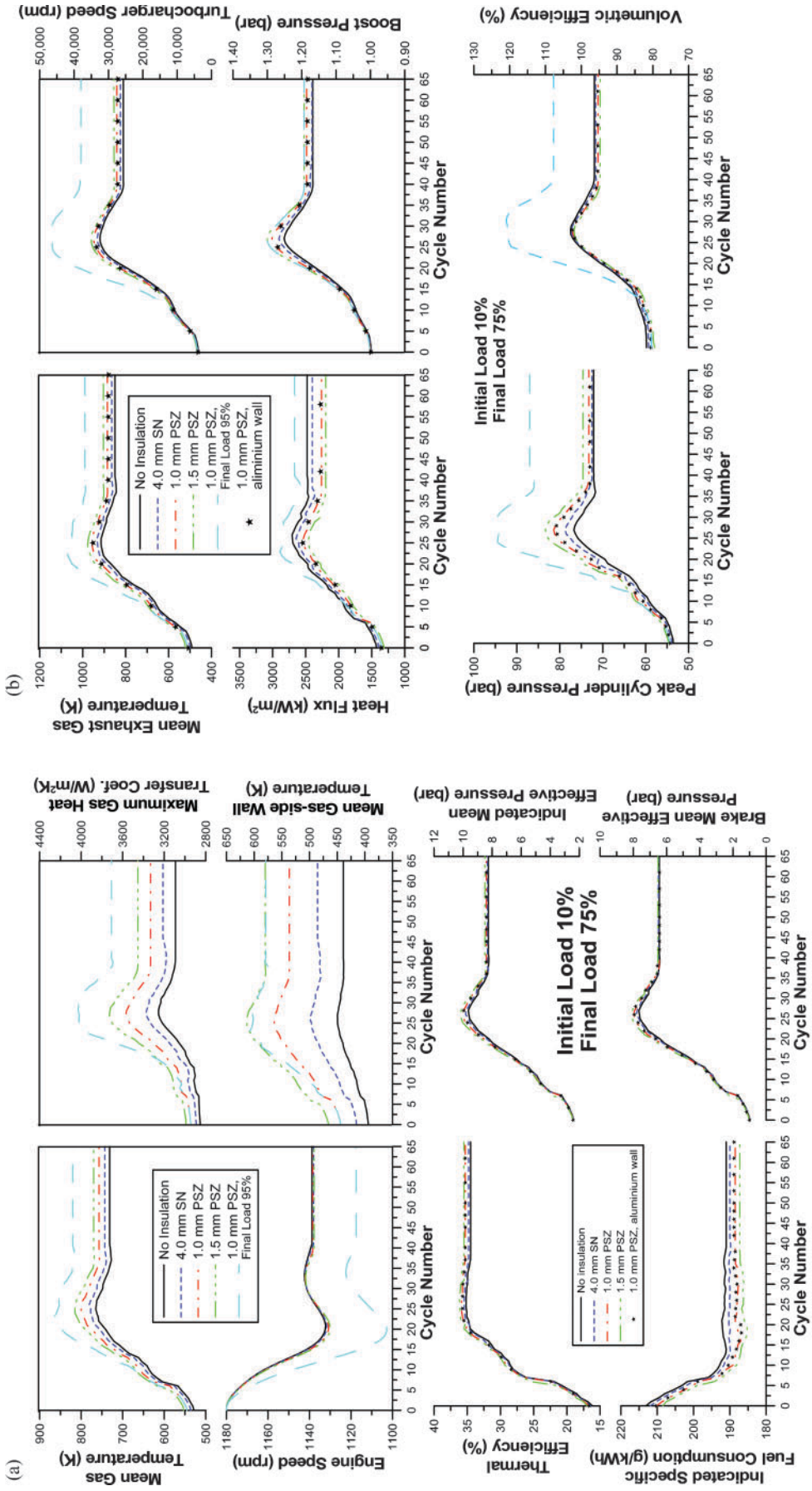

Fig. 4 Response of various engine and turbocharger properties to an increase in load (unless otherwise noted, the cylinder wall is cast iron and the load-change 10–75 per cent)

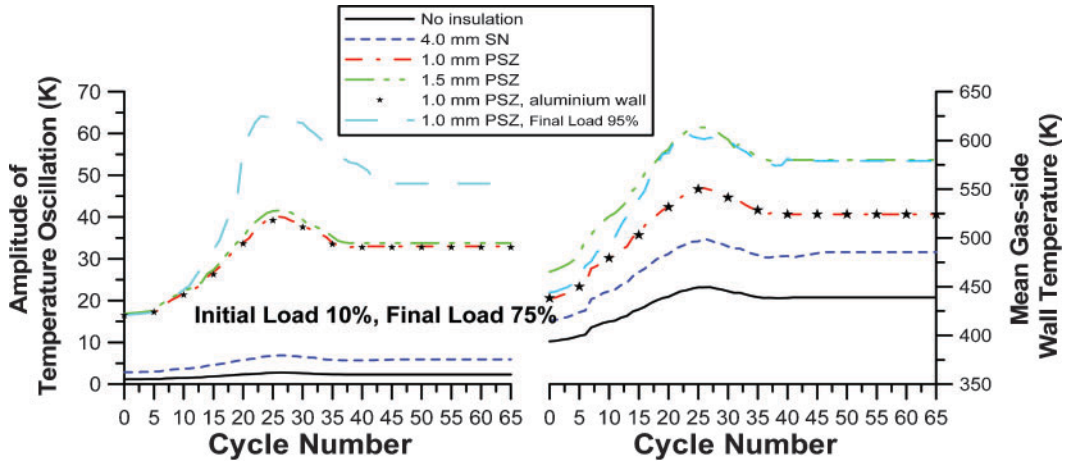

Fig. 5 Response of the temperature swing amplitude after a ramp increase in load, for various insulation schemes (unless otherwise noted, the cylinder wall is cast iron and the load-change 10–75 per cent)

5 RESULTS AND DISCUSSION

In Fig. 4(a), the upper four graphs illustrate the response of the engine speed and of three important parameters of the heat transfer mechanism, i.e. mean gas temperature, $\bar{T}_g$, mean gas-side wall temperature, $\bar{T}_{w,g}$, and maximum heat transfer coefficient from gas to cylinder wall, h_{max}. All the heat transfer variables depicted in these graphs agree with the results reached by Assanis and Heywood [**2**] for the steady state operation of a similarly rated turbocharged diesel engine. It is important to note that the engine speed is only slightly affected by the temperature levels inside the cylinder. This was also the result reached by Watson [**18**] and Schorn *et al.* [**22**], although these researchers did not investigate the effect of such a high level of insulation during transients. On the other hand, increasing the degree of insulation results in increased gas and wall temperatures throughout each cycle of the transient event, thus confirming the results reached by all other researchers for steady state operation. The latter finding, which was intuitively expected, discloses what the results should be if a second-law balance was applied. Increasing the temperature of the reactants, through insulation of the cylinder walls, significantly decreases the combustion irreversibilities, as the fuel chemical availability is now transferred to exhaust gases of higher temperature and thus work potential. Unfortunately, this decrease in availability destruction cannot be realized as an increase in piston work but rather as an increase in heat transfer to the cylinder walls and significant increase in the availability of the exhaust gases [**37**].

It is worth mentioning that although the heat transfer coefficient increases with increasing degree of insulation, as was expected due to the higher gas temperatures involved, the respective heat flux (middle left graph of Fig. 4(b)) exhibits the opposite behaviour. This is attributed to the reduced difference between gas and gas-side wall temperatures ($T_g - \bar{T}_{wg}$) when the insulation increases, a fact that can lead eventually to smaller requirements from the cooling system.

In Fig. 4(a), the four lower graphs expand the results of the previous paragraph by showing the response of the indicated specific fuel consumption (i.s.f.c.) and brake thermal efficiency of the engine in hand, highlighting the non-negligible benefit gained from the insulation. Increased temperature levels during each cycle lead to 'fuller' pressure diagrams, thus increasing the efficiency of the cycle up to 3.65 per cent for the 1.5 mm PSZ case at cycle 20 of the transient event. Clearly, the engine now handles the transient event slightly more efficiently. This confirms the results of Wong *et al.* [**10**], who reported an increase in engine efficiency with increasing temperature swings (cf. also remarks for Fig. 5 below, concerning the connection between degree of insulation and temperature swings). However, the increases in i.s.f.c. and, mainly, thermal efficiency are much smaller than would be expected judging from the corresponding increase in gas temperatures. Various theories have been proposed on the subject, with the most profound being the one proposed by Alkidas [**8**]. He argued that an increased level of insulation led to some kind of 'deterioration' of the combustion process by shifting a larger part of

the fuel burning into the diffusion phase, i.e. later in the cycle.

Following the efficiencies profile, the response of both i.m.e.p. and b.m.e.p. (lower right graph of Fig. 4(a)) is only slightly affected by the degree of insulation, with the highly insulated cases proving more favourable, mainly at those transient cycles where maximum fuelling is established. Here, the results are even less distinguished than the i.s.f.c. results. This is mainly due to the well-known fact of a decrease in the volumetric efficiency when increasing the degree of insulation, as will be explained in more detail later in this section.

The most notable effect of transient turbocharged diesel engine operation is the turbocharger lag [**20**]. This is pronounced with the continuous increase in engine rating, and it is usually realized with increased black smoke emissions. Turbocharger lag is caused because of the lack of mechanical connection between turbocharger compressor and engine crankshaft. Consequently, the power delivered to the turbine must first accelerate the turbocharger shaft in order for the compressor to be able to produce the increased boost pressure. Other related delays concern the use of fuel limiters, heat losses to the cylinder and exhaust manifold walls, and the acceleration of the rotating masses. Therefore, a higher wall temperature is generally expected to improve the turbocharger lag and thus speed response, as the effect of one of the above-mentioned 'decelerators' is considerably limited. This is actually the case here as suggested by the mean exhaust gas temperature response (upper left graph of Fig. 4b). Similar effects have been reported for the case where the exhaust manifold wall is insulated [**23**]. However, the improvement in turbocharger lag is not so pronounced for the present engine–load configuration, since its high total mass moment of inertia slows down the whole transient event. Consequently, the turbocharger operating point (identified through the boost pressure and turbocharger speed in the upper-right and mid-right graphs of Fig. 4(b)) differentiates only slightly with the degree of insulation compared with the uninsulated engine operation.

Closer examination of the curves in Fig. 4(b) reveals that the volumetric efficiency (based on atmospheric conditions) exhibits an interesting profile. Namely, a decreasing trend is observed with higher degree of insulation schemes. The increased level of cylinder wall temperatures during the induction process transfers heat to the incoming charge, thus reducing its density and hence

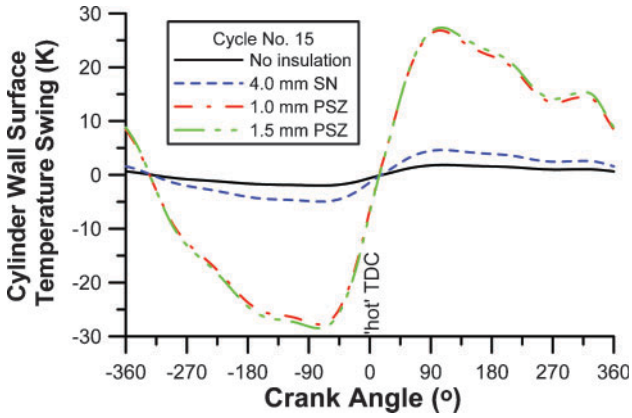

Fig. 6 Cylinder wall inside temperature oscillation swings against crank angle, for the various insulation schemes during an intermediate cycle (cycle number 15) of the transient load increase of 10–75 per cent

volumetric efficiency throughout the transient event. This behaviour is in agreement with the results reached by previous researchers for steady state operation.

For all properties studied, the difference between aluminium and cast iron wall (when both were coated with 1.0 mm PSZ) is modest. Obviously, it is the insulator's thermal properties that are primarily responsible for the decrease in the total thermal conductivity of the insulated cylinder wall that ultimately affects the engine's transient performance.

Figure 5 focuses on the short-term temperature oscillations during the transient event of the 10–75 per cent load-change, showing the response of the temperature swing amplitude; mean gas-side wall temperature response is also provided in this figure for comparison purposes. Whereas in the base, non-insulated, case the amplitude of the oscillation is about 2–3 K, values of up to 64 K at cycle 23 are noticed for the 10–95 per cent load-change when the engine is coated with 1.0 mm PSZ. These findings are in agreement with the results reached by Rakopoulos *et al.* [**12**, **13**] for steady state operation of a naturally aspirated diesel engine. Assanis and Heywood [**2**] reported even greater values for the amplitude of the temperature swing, but using a much lower thermal conductivity for the PSZ coating. From Fig. 5 it is also concluded that the increase from 1 to 1.5 mm PSZ has a rather modest effect on the temperature swing, whereas there is no practical difference between cast iron and aluminium walls. What should be mentioned here is the high rate of change of the swing amplitude between cycles 5 and 25, where the main part of the increased fuelling takes place. This rate, of the order of 4 K per cycle for the

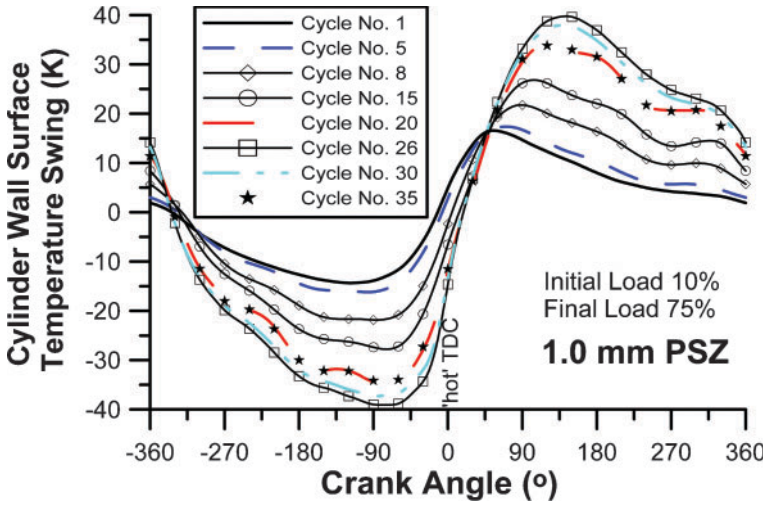

Fig. 7 Cylinder wall inside temperature oscillation swings against crank angle, for the insulation case of 1.0 mm PSZ, and for various cycles of the transient load increase of 10–75 per cent

10–95 per cent load-change or 2 K per cycle for the 10–75 per cent load-change for the insulated cases, is responsible for the increased thermal loading that is experienced by the engine structure during the transient event.

Figure 6 provides more detail of the cylinder inside wall temperature oscillation swings against crank angle, for the 15th cycle of the 10–75 per cent transient event. Likewise, Fig. 6 illustrates the same swings for various cycles of the transient event and for the case with 1.0 mm PSZ coating. These wall temperature oscillations increase with fuelling, as depicted in Fig. 7. However, their increase with the degree of insulation is forwarded at a decreasing rate [**12**, **13**]. This behaviour is explained in the following two paragraphs.

From equation (7) one can see that the wall temperature swing is proportional to the in-cylinder gas temperature levels (A_n, B_n) and a decreasing function of the parameter $\zeta^2 \propto k_{\text{ins}}^2/\alpha h^2$ (assuming a constant engine speed, i.e. constant $N = 1/\tau_o$, which for the transients presently examined is not a coarse approximation since, owing to the increased moment of inertia, small engine speed drops are observed). However, the variation of heat transfer coefficient with the degree of insulation is very mild [**12**, **13**], so that effectively $\zeta^2 \propto k_{\text{ins}}^2/\alpha$. Values of k_{ins}^2/α are calculated as follows for cast iron, silicon nitride, and PSZ, respectively: 2.1×10^8, 0.36×10^8, and 0.11×10^8. Thus, ζ^2 is a decreasing function of the degree of insulation. The strong increase of the wall temperature swing with the degree of insulation can then be explained by both the higher gas temperatures (cf. Fig. 4) and the lower values of ζ^2. Nonetheless, this increase with the degree of insulation is forwarded at a decreasing rate. This is explained by the fact that, at high degrees of insulation (e.g. for the zirconia cases), the value of ζ^2 becomes very small with respect to 1. Then, the influence on the wall temperature swing value derives effectively only from the relatively milder increase of the gas temperature swing with the degree of insulation.

The explanation for the behaviour observed with fuelling (Fig. 7) is as follows. Again from equation (7) it can be seen that the wall temperature swing is proportional to a decreasing function of parameter $\zeta^2 \propto 1/h^2$ (for a specific speed, i.e. constant $N \propto 1/\tau_o$, and for the same wall material, i.e. constant k_{ins} and α). From equation (7) it can also be seen that the wall temperature swing phase shifting is an increasing function of parameter ζ. The strong increase of the wall temperature swing with fuelling as the transient event develops can then be explained by both the higher gas temperatures and gas heat transfer coefficients (i.e. lower ζ) (cf. Fig. 4).

From Figs 6 and 7 it can also be observed that the temperature gradients appear more pronounced the higher the fuelling or the degree of insulation. Figure 8 illustrates the 'wave' of temperature variations inside the cylinder wall for four discrete cycles of the 10–75 per cent transient event (cycle number 26 corresponds to the maximum fuelling), and for the case with 1.0 mm PSZ coating. Figure 9 expands on the temperature swing development, depicting the response of the crank angle where the maximum value (that depicted in Fig. 5) is observed as well as the depth where the swing dies out. As the transient event develops, the governor responds to the initial speed decrease, increasing the fuelling considerably in order for the engine to cope with the higher

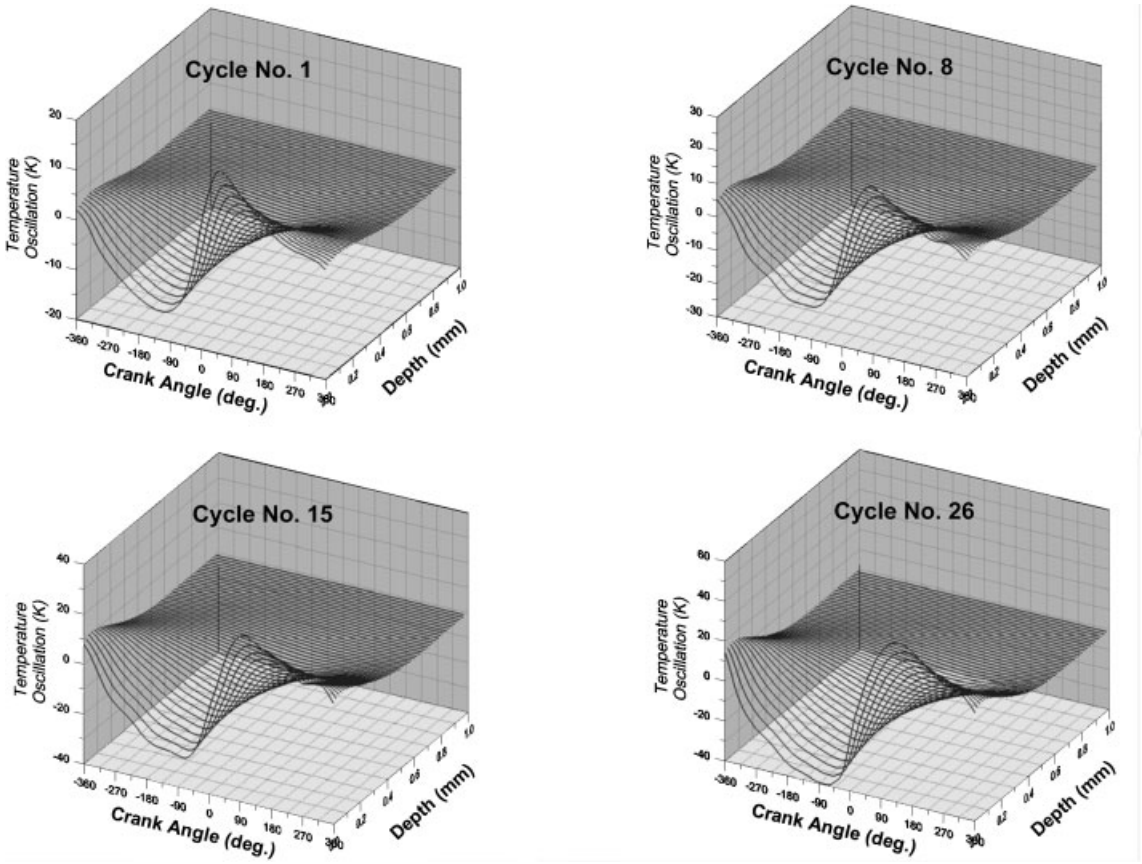

Fig. 8 Variation of wall temperature with depth x (inside the wall) and crank angle φ, for the insulation case of 1.0 mm PSZ, and for four discrete cycles of the transient load increase of 10–75 per cent

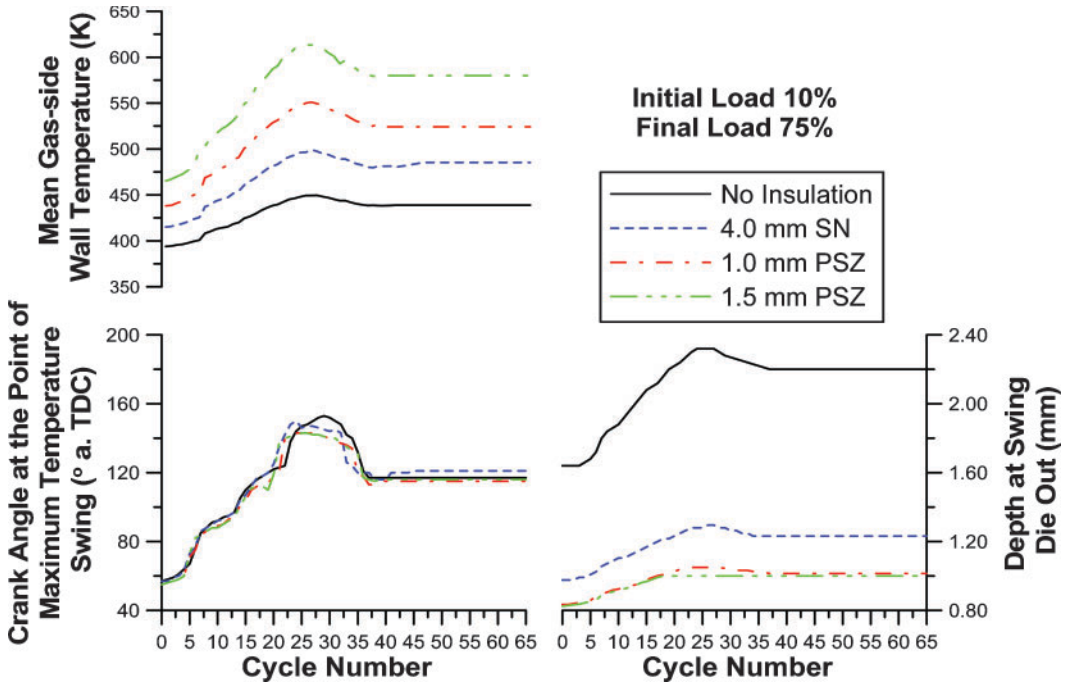

Fig. 9 Response of crank angle at the point of maximum temperature swing and depth where swing dies out after a ramp increase in load, for various insulation schemes

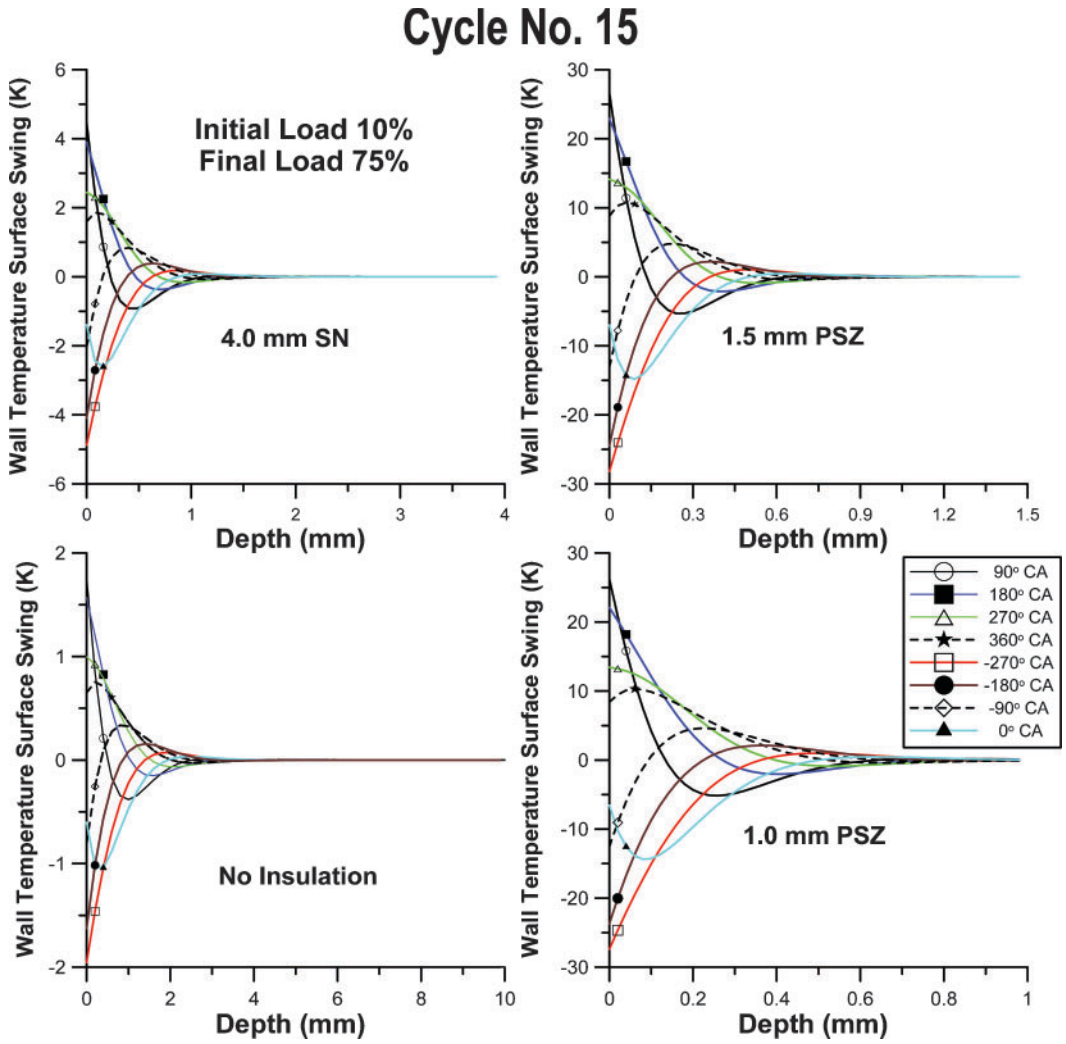

Fig. 10 Variation of wall temperature swings with depth x (inside the wall) extending over a wavelength, at various crank angles, for the various insulation schemes during an intermediate cycle (cycle number 15) of the transient load increase of 10–75 per cent

loading. This leads to higher values of flame temperatures and an increased duration of combustion, which gradually shifts the crank angle at which the maximum swing is observed later in the cycle (cf. also Fig. 7). The respective crank angle at the point of maximum heat transfer coefficient is around 'hot' TDC, whereas the crank angle where the maximum cylinder temperature occurs is 40° CA after TDC owing to the indirect type of the injection for the engine in hand. The type of insulation is of much lesser importance here, as all the graphs corresponding to the 10–75 per cent load-change show the same profile. Similarly, the increased fuelling and gas temperatures lead to a greater penetration depth of the observed temperature swings. Similar to the results reached in references [**2**], [**12**], and [**13**] during steady state engine operation, the heavy insulated cases exhibit a smaller depth of penetration thus substantially increasing the thermal shock. This can be explained by noting that in these cases the temperature amplitude is increased while at the same time the penetration depth is decreased, i.e. the gradients are increased.

The latter is explained in more detail in Fig. 10, which shows the variation of wall temperature swings with depth x (inside the wall) extending over a wavelength x_o, at various crank angles (instants of time) extending over the current engine cycle period τ_o (corresponding to 720° CA), at the 15th engine cycle of the 10–75 per cent transient event. Profiles of similar type develop during all the other cycles of the transient event. The strong damping of the wall temperature swings with depth x is apparent. Effectively, the wall swings disappear at a depth of the order of 0.6–3 mm. It can clearly be seen that when increasing the degree of insulation the amplitude of

the wall temperature swings highly increases while, at the same time, the corresponding depths inside which they disappear decrease (cf. Fig. 9). The first effect has been explained during the discussion of Fig. 7. The decrease of depth inside which these oscillations disappear, when increasing the degree of insulation, is explained by noting from equation (9) that the related wavelength $x_o \propto \alpha^{1/2}$, with α decreasing in value with the degree of insulation increase. The combination of large temperature gradients with short penetration lengths, as for example in the zirconia insulation cases, results in high thermal gradients, thus leading to high cyclic thermal loading. Therefore, the material concerned should possess high fatigue durability and thermal shock resistance as well as good temperature strength [**6**, **21**].

6 CONCLUSION

An experimentally validated transient diesel engine simulation code has been extended to include a detailed heat transfer analysis applying Fourier techniques. The model is used to investigate the effect of engine wall materials of special technological importance, such as the well-known insulators silicon nitride or PSZ, on the values of cyclic temperature swings and engine performance during transients.

Detailed diagrams provide a comparison of engine performance with these materials as against the baseline performance corresponding to the usual engine wall materials, e.g. cast iron. For the present engine–load configuration the analysis revealed the following points.

1. An increased degree of insulation during a typical transient load increase, of the order of 10–75 per cent, resulted in increased gas and wall temperatures, heat transfer coefficients, and, mainly, amplitude of temperature swings and temperature gradients. The latter may take prohibitive values causing severe wall thermal fatigue, so that proper care should be taken regarding the thermal stress of the engine components.
2. The transient response of the engine exhibits a behaviour that goes along with the respective steady state performance. Namely, the higher temperature levels observed throughout the cycle result in decreased volumetric efficiency and slightly improved indicated efficiency. The main finding for the particular engine–load set-up was the rather unaffected, by the level of applied insulation, response of all engine and turbocharger non-heat-transfer-related values, with the latter attributed to the high moment of inertia of the current engine–load configuration, which slows down the transient response.
3. No significant distinction was noticed between cast iron and aluminium walls as regards engine transient response.

It is the intention of the present research group to proceed to experimental validation in the near future concerning the above-mentioned predicted results, at least as regards the short-term, gas-side, cylinder wall temperature oscillations during transients.

REFERENCES

1 **Annand, W. J. D.** and **Ma, T. H.** Instantaneous heat transfer rates to the cylinder head surface of a small compression-ignition engine. *Proc. Instn Mech. Engrs*, 1970–71, **185**, 976–987.

2 **Assanis, D. N.** and **Heywood, J. B.** Development and use of a computer simulation of the turbocompounded diesel engine performance and component heat transfer studies. SAE paper 860329, 1986.

3 **Borman, G.** and **Nishiwaki, K.** Internal-combustion engine heat transfer. *Prog. Energy Combust. Sci.*, 1987, **13**, 1–46.

4 **Benson, R. S.** and **Whitehouse, N. D.** *Internal combustion engines*, 1979 (Pergamon Press, Oxford).

5 **Heywood, J. B.** *Internal combustion engine fundamentals*, 1988 (McGraw-Hill, New York).

6 **Bryzik, W.** and **Kamo, R.** Tacom/Cummins adiabatic engine program. SAE paper 830314, 1983.

7 **Woschni, G.** and **Spindler, W.** Heat transfer with insulated combustion chamber walls and its influence on the performance of diesel engines. *Trans. ASME, J. Engng Gas Turbines Power*, 1988, **110**, 482–488.

8 **Alkidas, A. C.** Performance and emissions achievements with an uncooled heavy-duty, single-cylinder diesel engine. SAE paper 890144, 1989.

9 **Assanis, D., Wiese, K., Schwartz, E.,** and **Bryzik, W.** The effects of ceramic coatings on diesel engine performance and exhaust emissions. SAE paper 910460, 1991.

10 **Wong, V. W., Bauer, W., Kamo, R., Bryzik, W.,** and **Reid, M.** Assessment of thin thermal barrier coatings for I.C. engines. SAE paper 950980, 1995.

11 **Rakopoulos, C. D.** and **Mavropoulos, G. C.** Modelling the transient heat transfer in the ceramic combustion chamber walls of a low heat rejection diesel engine. *Int. J. Vehicle Design*, 1999, **22**, 195–215.

12 **Rakopoulos, C. D., Antonopoulos, K. A., Rakopoulos, D. C.,** and **Giakoumis, E. G.** Investigation

of the temperature oscillations in the cylinder walls of a diesel engine with special reference to the limited cooled case. *Int. J. Energy Res.*, 2004, **28**, 977–1002.

13 **Rakopoulos, C. D., Rakopoulos, D. C., Mavropoulos, G. C.,** and **Giakoumis, E. G.** Experimental and theoretical study of the short term response temperature transients in the cylinder walls of a diesel engine at various operating conditions. *Appl. Thermal Engng*, 2004, **24**, 679–702.

14 **Alkidas, A. C.** and **Myers, J. P.** Transient heat-flux measurements in the combustion chamber of a spark-ignition engine. *Trans. ASME, J. Heat Transfer*, 1982, **104**, 62–67.

15 **Alkidas, A. C.** and **Cole, R. M.** Transient heat-flux measurements in a divided-chamber Diesel engine. *Trans. ASME, J. Heat Transfer*, 1985, **107**, 439–444.

16 **Rakopoulos, C. D.** and **Mavropoulos, G. C.** Experimental instantaneous heat fluxes in the cylinder head and exhaust manifold of an air-cooled diesel engine. *Energy Convers. Mgmt*, 2000, **41**, 1265–1281.

17 **Zhao, H.** and **Ladommatos, N.** *Engine combustion instrumentation and diagnostics*, 2001 (Society of Automotive Engineers Inc., Warrendale, Pennsylvania).

18 **Watson, N.** Dynamic turbocharged diesel engine simulator for electronic control system development. *Trans. ASME, J. Dynamic Syst. Measmt Control*, 1984, **106**, 27–45.

19 **Winterbone, D. E.** Transient performance. In *The thermodynamics and gas dynamics of internal combustion engines* (Eds J. H. Horlock and D. E. Winterbone), vol. II, 1986 (Clarendon Press, Oxford).

20 **Rakopoulos, C. D.** and **Giakoumis, E. G.** Review of thermodynamic diesel engine simulations under transient operating conditions. SAE paper 2006-01-0884. Also *Trans. SAE, J. Engines*, 2006, **115**, 467–504.

21 **Keribar, R.** and **Morel, T.** Thermal shock calculations in I.C. engines. SAE paper 870162, 1987.

22 **Schorn, N., Pischinger, F.,** and **Schulte, H.** Computer simulation of turbocharged diesel engines under transient conditions. SAE paper 870723, 1987.

23 **Rakopoulos, C. D., Giakoumis, E. G., Hountalas, D. T.,** and **Rakopoulos, D. C.** The effect of various dynamic, thermodynamic and design parameters on the performance of a turbocharged diesel engine operating under transient load conditions. SAE paper 2004-01-0926, 2004.

24 **Arcoumanis, C., Chan, S. H.,** and **Bazari, Z.** Optimisation of the transient performance of a turbocharged diesel engine using turbocharging and fuel injection control. In IMechE Seminar on *Engine transient performance*, 1990, pp. 13–26 (Institution of Mechanical Engineers, London).

25 **Arcoumanis, C., Megaritis, A.,** and **Bazari, Z.** Analysis of transient exhaust emissions in a turbocharged vehicle diesel engine. In IMechE Conference on *Turbocharging and turbochargers*, 1994, Paper C484/038, pp. 71–81 (Institution of Mechanical Engineers, London).

26 **Rakopoulos, C. D.** and **Giakoumis, E. G.** Simulation and analysis of a naturally aspirated, indirect injection diesel engine under transient conditions comprising the effect of various dynamic and thermodynamic parameters. *Energy Convers. Mgmt*, 1998, **39**, 465–484.

27 **Rakopoulos, C. D.** and **Giakoumis, E. G.** Sensitivity analysis of transient diesel engine simulation. *Proc. IMechE, Part D: J. Automobile Engineering*, 2006, **220**, 89–101.

28 **Rakopoulos, C. D., Hountalas, D. T., Mavropoulos, G. C.,** and **Giakoumis, E. G.** An integrated transient analysis simulation model applied in thermal loading calculations of an air-cooled diesel engine under variable speed and load conditions. SAE paper 970634, 1997. Also *Trans. SAE, J. Engines*, 1997, **106**, 923–939.

29 **Rakopoulos, C. D., Hountalas, D. T.,** and **Mavropoulos, G. C.** Modelling the structural thermal response of an air-cooled diesel engine under transient operation including a detailed thermodynamic description of boundary conditions. SAE paper 981024, 1998.

30 **Whitehouse, N. D.** and **Way, R. G. B.** Rate of heat release in diesel engines and its correlation with fuel injection data. *Proc. Instn Mech. Engrs, Part J*: 1969–70, 184, 17–27.

31 **Gebhart, B.** *Heat transfer*, 1971 (McGraw-Hill, New York).

32 **Myers, G. E.** *Analytical methods in conduction heat transfer*, 1971 (McGraw-Hill, New York).

33 **Eckert, E. R. G.** and **Drake Jr, R. M.** *Heat and mass transfer,* Second Edition, 1959 (McGraw-Hill, New York).

34 **Churchill, R. V.** *Fourier series and boundary value problems*, 1963 (McGraw-Hill, New York).

35 **Rakopoulos, C. D.** and **Hountalas, D. T.** A simulation analysis of a DI diesel engine fuel injection system fitted with a constant pressure valve. *Energy Convers. Mgmt*, 1996, **37**, 135–150.

36 **Taraza, D., Henein, N.,** and **Bryzik, W.** Friction losses in multi-cylinder diesel engines. SAE paper 2000-01-0921, 2000.

37 **Rakopoulos, C. D.** and **Giakoumis, E. G.** Second-law analyses applied to internal combustion engine operation. *Prog. Energy Combust. Sci.*, 2006, **32**, 2–47.

APPENDIX

Notation

A	surface area (m^2)
G	mass moment of inertia ($kg\,m^2$)
h	heat transfer coefficient ($W/m^2\,K$)
k	thermal conductivity ($W/m\,K$)

m	mass (kg)
n	order of harmonic component (Fourier coefficient)
N	engine speed (r/min)
Q	heat loss (J)
S	layer thickness (m)
T	absolute temperature (K)
t	time (s)
V	volume (m^3)
x	distance (inwards) from the cylinder inside wall surface (m)
α	thermal diffusivity (m^2/s)
τ	period (s)
φ	crank angle measured from the firing ('hot') top dead centre position (deg)
ω	angular velocity (rad/s)

Abbreviations

°CA	degrees crank angle
BDC	bottom dead centre
PSZ	plasma spray zirconia
SMD	Sauter mean diameter (m)
SN	silicon nitride
TDC	top dead centre

Subscripts

c	coolant
e	engine
g	gas
ins	insulation
m	insulation–cylinder wall interface
p	periodic
w	wall